A geometric Brownian motion car-following model towards a better understanding of capacity drop

Yuan, Kai; Lavala, Jorge; Knoop, Victor; Jiang, Rui; Hoogendoorn, Serge

DOI
10.1080/21680566.2018.1518169

Publication date
2018

Document Version
Final published version

Published in
Transportmetrica B: Transport Dynamics

TRANSPORTMETRICA B: TRANSPORT DYNAMICS
https://doi.org/10.1080/21680566.2018.1518169

Taylor & Francis
Taylor & Francis Group

A geometric Brownian motion car-following model: towards a better understanding of capacity drop

K. Yuan[a,b], Jorge Laval[a], Victor L. Knoop[b], Rui Jiang[c] and Serge P. Hoogendoorn [b]

[a]School of Civil and Environmental Engineering, Georgia Institute of Technology, Atlanta, GA, USA; [b]Department of Transport and Planning, Faculty of Civil Engineering and Geosciences, Delft University of Technology, Delft, Netherlands; [c]MOE Key Laboratory for Urban Transportation Complex Systems Theory and Technology, Beijing Jiaotong University, Beijing, People's Republic of China

ABSTRACT

Traffic flow downstream of the congestion is generally lower than the pre-queue capacity. This phenomenon is called the capacity drop. Recent empirical observations show a positive relationship between the speed in congestion and the queue discharge rate. Literature indicates that variations in driver behaviors can account for the capacity drop. However, to the best of authors' knowledge, there is no solid understanding of what and how this variation in driver behaviors lead to the capacity drop, especially without lane changing. Hence, this paper fills this gap. We incorporate the empirically observed desired acceleration stochasticity into a car-following model. The extended parsimonious car-following model shows different capacity drop magnitudes in different traffic situations, consistent with empirical observations. All results indicate that the stochasticity of desired accelerations is a significant reason for the capacity drop. The new insights can be used to develop and test new measures in traffic control.

ARTICLE HISTORY
Received 27 June 2017
Accepted 25 July 2018

KEYWORDS
Traffic flow; capacity drop; car-following model; intra-driver variation

1. Introduction

It is generally agreed that the capacity drop phenomenon is the salient feature of freeway bottlenecks: once congestion occurs, the queue discharge rate is 5–20% lower than the pre-queue capacity (Banks 1991; Hall and Agyemang-Duah 1991; Cassidy and Bertini 1999; Cassidy and Rudjanakanoknad 2005; Chung, Rudjanakanoknad, and Cassidy 2007; Srivastava and Geroliminis 2013). Recent empirical findings by Yuan, Knoop, and Hoogendoorn (2015) show yet another reproducible phenomenon, that the queue discharge rate increases with the speed in the queue; see Figure 1. In this figure, the capacity drop magnitude is around 26% when the vehicular speed in congestion is zero km/h and decreases as the vehicular speed increases. The mechanisms behind this "speed-capacity" relationship are not well understood, to the detriment of traffic operations, simulation models and traffic delay calculations. This paper aims to fill this void.

Laval and Daganzo (2006) demonstrate that the disruption caused by some lane-changing maneuvers near merge and moving bottlenecks might explain capacity drop; see also Yeo (2008), Coifman and Kim (2011), Leclercq, Laval, and Chiabaut (2011), Leclercq et al. (2015), Yuan et al. (2017b), and Yuan, Knoop, and Hoogendoorn (2015). This disruption takes the form of a void in traffic in front of the lane-changing vehicle, which is caused by the bounded acceleration of the maneuver.

CONTACT K. Yuan spidermanyuan@gmail.com

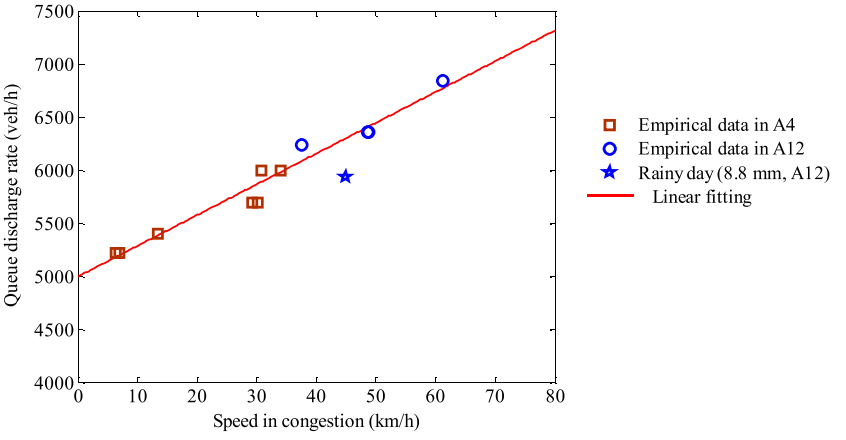

Figure 1. Relation between the speed in congestion (v_j) and the queue discharge rate (q_{dis}) (Yuan, Knoop, and Hoogendoorn 2015). The data are loop detector data collected on three-lane sections on two freeways, A4 and A12, in the Netherlands. The speed in congestion is the average of detected speed in a spatial-temporal region where congestion is observed. The flow is calculated using slanted cumulative curves in the downstream of congestion. Both detected locations are flat and almost straight. More explicit descriptions are referred to Yuan, Knoop, and Hoogendoorn (2015) and Yuan (2016). Except one data point (shown as a star), all data are collected in sunny days. When fitting the data, the data collected in the rainy day is excluded. The linear fitting function is $q_{\text{dis}} = 29 \cdot v_j + 5000$.

However, recent observations reveal that capacity drop can also take place in the absence of lane changing (Oh and Yeo 2015). This suggests that voids can form between any two successive vehicles rather than only in the front of lane changers. After analyzing time headways in the downstream free-flow state of congestion in the absence of lane changing, Oh and Yeo (2015) also find that the queue discharge rate decreases as the congestion severity increases, which is consistent with the speed-capacity relationship from Yuan, Knoop, and Hoogendoorn (2015). It has been argued that the driver–vehicle-combination (DVC) heterogeneity might explain this phenomenon. Wong and Wong (2002) suggested that the variance of drivers' desires for free-flow speeds might be a reason for the capacity drop. They extend the LWR model (Lighthill and Whitham 1955; Richards 1956) to incorporate a distribution of fundamental diagrams characterized by their choices of speeds in a traffic stream, and obtain a reverse-lambda fundamental diagram within simulations. However, a behavioral explanation and empirical data for this conjecture are still lacking. Chen et al. (2016) study the effect of heavy vehicles on driver behaviors through empirical analysis and find that heavy vehicles might reduce capacity drop by stabilizing surrounding traffic streams, but caution that more data is needed to confirm their findings. Coifman (2015) show the impacts of the DVC heterogeneity on the fundamental diagram, but no conclusion on the capacity drop is drawn.

Two other mechanisms have been proposed for explaining capacity drop (see Yuan, Knoop, and Hoogendoorn 2017a, for a summary): inter-driver spread (Papageorgiou et al. 2008) and the intra-driver variation (Tampère 2004; Zhang and Kim 2005; Treiber, Kesting, and Helbing 2006; Chen et al. 2014; Yuan, Knoop, and Hoogendoorn 2017a). The inter-driver spread means heterogeneity in the desired accelerations, e.g. voids can be created between a low-acceleration vehicle and its high-acceleration predecessor, as noted in Laval and Daganzo (2006). Yuan, Knoop, and Hoogendoorn (2017a) find that the queue discharge rate reduction due to the acceleration spread is rather small compared to the bounded acceleration component.

The intra-driver variation mechanism means that the capacity drop is a result of traffic condition dependent variable driver behavior. For example, Zhang and Kim (2005) assume the driver gap-time as a function of both gap-distance and traffic phase. Treiber, Kesting, and Helbing (2006) investigate an adaption of desired time headway as a function of local speed variances. However, in these models, a proper understanding of the capacity drop from a behavioral perspective is missing. The

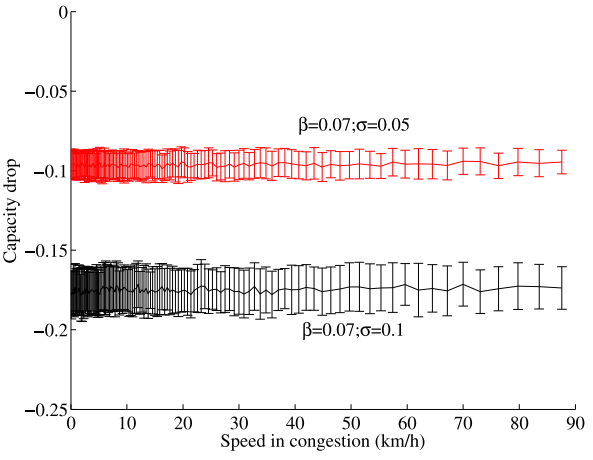

Figure 2. Relation between the speed in congestion and the capacity drop given by the parsimonious car-following model. The error bar indicates the standard deviation of the capacity drop. β and σ are two constant parameters in the model. A higher σ gives a larger capacity drop.

timid-aggressive models (Laval and Leclercq 2010; Chen et al. 2014, 2012a, 2012b) modify Newell's first-order car-following model (Newell 2002) to incorporate both bounded accelerations and different reaction patterns to disturbances to replicate realistic oscillations formation and propagation. The drawback of this formulation is that several extra parameters are needed, which might be difficult to estimate in real applications. Laval, Toth, and Zhou (2014) propose a stochastic extension to Newell's car-following model with bounded accelerations requiring a single extra parameter and exhibiting a predicted ability similar to the timid/aggressive models.

Based on the above discussions, it seems reasonable that the parsimonious model in Laval, Toth, and Zhou (2014) might explain the speed-capacity relationship in Figure 1. Unfortunately, this is not the case as shown in Figure 2. The inability of the model in Laval, Toth, and Zhou (2014) to reproduce the bottlenecks speed-discharge rate relationship raises the question whether the stochasticity in driver behaviors is associated with the capacity drop phenomenon, and if so, in which way. In this paper, we answer this question by showing an alternative formulation of the model in Laval, Toth, and Zhou (2014) based on additional empirical data analysis. An explicit driver behavioral mechanism behind the capacity drop phenomenon is developed here, which is expected to shed light on traffic operations. Towards this end, the outline of the paper is as follows: we present the extended car-following model in Section 2. The power of the car-following model over showing longitudinal drivers' behaviors is investigated in Section 3, with comparisons to earlier empirical findings. Section 3 simulates the capacity drop and its relation with congestion states using the extended model. Finally, we end this paper with conclusions and discussions in Section 4.

2. The car-following model

This section formulates the proposed car-following model, which is based on the concept of desired acceleration. The desired acceleration is defined as the acceleration drivers are willing to impose on their vehicles in the absence of a leader.

Figure 3 shows the desired acceleration at different vehicular speeds. These data include 15 acceleration processes by the *same* driver, which are collected only when the test vehicle is the first one in a platoon stopped in front of the red signal. The data is the same as analyzed in Laval, Toth, and Zhou (2014). Figure 3(b) shows that the standard deviation of the desired accelerations almost reduces linearly as the vehicular speed grows. The points in Figure 3(b) are given by calculating the standard

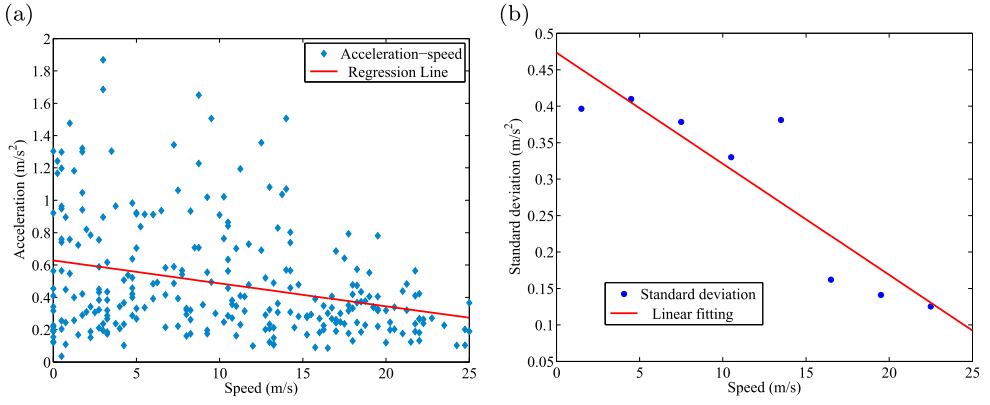

Figure 3. Data collections for justifying the function between the vehicular speed and the desired accelerations. (a) Vehicular speed and desired accelerations from 15 experiments in Laval, Toth, and Zhou (2014), collected when the test vehicle is the platoon leader stopped in front of a red signal. A regression line $a(v(t)) = -0.014v(t) + 0.63$ is used to fit the data with $R^2 = 0.0876$ (b) Standard deviation of the desired accelerations in 5-m/s speed bins. A linear function $\text{Std}(a(v(t))) = 0.015v(t) + 0.47$ is applied to fit the data in Figure 3(b). (a) Drivers' desired acceleration when traveling at different speed. (b) Standard deviation of drivers' desired accelerations at different vehicular speeds *v*.

deviation of an aggregation of points in an interval of 3 m/s. This observed dependency between standard deviation and speed was overlooked in the model proposed in Laval, Toth, and Zhou (2014), and we will see that it might be the reason why this model cannot capture the speed-capacity relationship. One may argue that using a linear function to fit the trend shown in Figure 3 may not be accurate. But we would argue that the overall decreasing trend shown in Figure 3 is consistent with real driving features as observed in Allen et al. (2000), and is a key ingredient to predict realistic traffic dynamics. In the future, to what extent the linearity assumption might influence the results should be investigated.

We now show that this stochastic feature during accelerating is relevant for reducing queue discharge rates, and can be incorporated into the model by using a geometric Brownian motion to describe desired accelerations. We firstly introduce a stochastic desired acceleration model that is consistent with empirical data in Section 2.1, and then it is incorporated into Newell's first-order car-following framework in Section 2.2. Finally, a single-parameter model is given in Section 2.3

2.1. The desired acceleration model

In this section we formulate the desired acceleration model, which corresponds to the acceleration processes of a single driver on an empty road, only constrained by the engine power and the way the driver uses it. Using empirical data, Laval, Toth, and Zhou (2014) show that the following linear vehicle kinematics model is a good approximation for the mean desired acceleration $\text{E}[a(v)]$ when a vehicle is traveling at speed $v(t)$ at time t, i.e.

$$\text{E}[a(v(t))] = (v_f - v(t))\beta \tag{1}$$

where v_f is the free-flow speed and β is a positive parameter with units of $[\text{time}]^{-1}$. (1) is also consistent with linearized relaxation acceleration model in Treiber, Hennecke, and Helbing (2000) and Treiber, Kesting, and Helbing (2006). Laval, Toth, and Zhou (2014) assume that the desired acceleration is normally distributed around this mean with constant standard deviation, $\text{Std}[a(v(t))]$, independent of the speed. However, we found that further analysis of the empirical data in that reference reveals that $\text{Std}[a(v(t))]$ decrease with the speed $v(t)$; this is shown in Figure 3(b). It can be seen that the mean and standard deviation are linear functions of the speed, both of which vanish near v_f. This suggests that the following stochastic differential equation (SDE) should be a good approximation:

$$\text{d}v(t) = (v_f - v(t))\beta\text{d}t + (v_f - v(t))\sigma\text{d}W(t) \tag{2}$$

where $W(t)$ is the standard Brownian motion and σ is diffusion coefficient, which has units of [time]$^{-1/2}$. Using $S(t) = v_f - v(t)$, we reformulate (2) into

$$\mathrm{d}S(t) = -S(t)(\beta \mathrm{d}t + \sigma \mathrm{d}W(t)) \tag{3}$$

with initial conditions $S(0) = S_0$, with $S_0 = v_f - v_0$ and $v_0 = v(0)$. It is noted that in simulations, the initial state is the state in the last simulation instant rather than the traffic condition at the beginning of the simulation. That is, as shown in Zhang, Wu, and Wong (2012) and Wu et al. (2014), similar to the many existing car-following models, the car-following model in this paper takes the current traffic states into account.

SDE (3) indicates that the stochastic process $S(t)$ follows a Geometric Brownian motion, and therefore, under Itō's interpretation of SDEs (Øksendal 2010), obeys a log-normal distribution with expected value $\mathrm{E}[S(t)] = S_0 e^{-\beta t}$ and variance $\mathrm{Var}[S(t)] = S_0^2 e^{-2\beta t}(e^{\sigma^2 t} - 1)$. Hence, $v(t)$ follows log-normal distribution with E[·] and Var[·] given by:

$$\mathrm{E}[v(t)] = v_f - (v_f - v_0)\mathrm{e}^{-\beta t} \tag{4a}$$

$$\mathrm{Var}[v(t)] = (v_f - v_0)^2(\mathrm{e}^{-(2\beta - \sigma^2)\, t} - \mathrm{e}^{-2\beta t}) \tag{4b}$$

Note that log-normality here means that $v(t)$ is always non-negative. To identify the parameters that drive the model, consider the dimensionless quantities $\tilde{\sigma}^2 = \sigma^2/\beta$, $\tilde{t} = \beta t$ and $\tilde{v} = v/v_f$, which simplify (4) into:

$$\mathrm{E}[\tilde{v}(\tilde{t})] = 1 - (1 - \tilde{v}_0)\mathrm{e}^{-\tilde{t}} \tag{5a}$$

$$\mathrm{Var}[\tilde{v}(\tilde{t})] = (1 - \tilde{v}_0)^2(\mathrm{e}^{-(2-\tilde{\sigma}^2)\, \tilde{t}} - \mathrm{e}^{-2\tilde{t}}) \tag{5b}$$

which reveals that apart from the initial data $\tilde{v}_0$ the only parameter in the model is $\tilde{\sigma}^2$. Notice how the steady-state speed variance tends to zero if $\tilde{\sigma}^2 \leq 2$ (and to infinity otherwise), which should always be the case in practice as we will see momentarily.

2.2. Incorporation into car-following framework

Here we incorporate the desired acceleration model (4) into the Newell's first-order car-following framework (2002). Newell's model can be expressed as:

$$x_{i+1} = \min\{x_{i+1}(t - \tau) + \tau v_f, x_i(t - \tau) - \delta\} \tag{6}$$

where $\delta = 1/\rho_j$. $x_i(t)$ is the location of vehicle i at time t and $\tau = 1/(w\rho_j)$ is the wave travel time between two successive vehicles. The jam density ρ_j, shock wave speed $-w$ and free-flow speed v_f are three parameters of a triangular flow-density fundamental diagram, from which the capacity and critical density associated with the fundamental diagram can be derived.

Remark here the speed generation via (4) or (5) in this research may result in a speed higher than the free-flow speed v_f. To incorporate the $v(t)$ in to (6), the term τv_f is reformulated into $\tau \cdot \min(v_f, v_{i+1}(t))$. That is:

$$x_{i+1}(t) = \min\{x_{i+1}(t - \tau) + \tau \cdot \min(v_f, v_{i+1}(t)), x_i(t - \tau) - \delta\} \tag{7}$$

where the $v_{i+1}(t)$ term in (7) is obtained by generating a log-normal random number with mean value and variance given by (4). Recall that the log-normal distribution ensures$v(t)$ is always non-negative. The formulation of (7) may make an assumption that the acceleration vanishes at free-flow, which might be not fully realistic. Readers can relax this assumption by formulating (7) as $x_{i+1}(t) = \min\{x_{i+1}(t - \tau) + \tau \cdot v_{i+1}(t), x_i(t - \tau) - \delta\}$ which allows $v_{i+1}(t) > v_f$.

2.3. A single-parameter model

It is important to note that it has been shown that, in the context of the kinematic wave model, the parameters added by the fundamental diagram (τ, v_f and δ in our case) do not impact flow or delay calculations, when expressed in dimensionless form (Laval, Toth, and Zhou 2014; Daganzo and Knoop 2016; Laval and Chilukuri 2016).

It follows that that capacity drop should be a function of $\tilde{\sigma}^2$ alone, since we have seen that this is the only additional parameter required by our model. The numerical experiments in the next section confirm this result.

3. Simulation experiments

This section presents two simulation experiments with the proposed model. The results are consistent with empirical data, at the aggregate level. In both cases the experiment consists of a platoon on a single lane and without lane changes.

The triangular fundamental diagram has parameters $w = 18$ km/h, $v_f = 114$ km/h, and free-flow capacity $C = 2280$ veh/h. Accordingly, $\rho_j \approx 146.7$ veh/km and critical density $\rho_{\text{cri}} = 20$ veh/km.

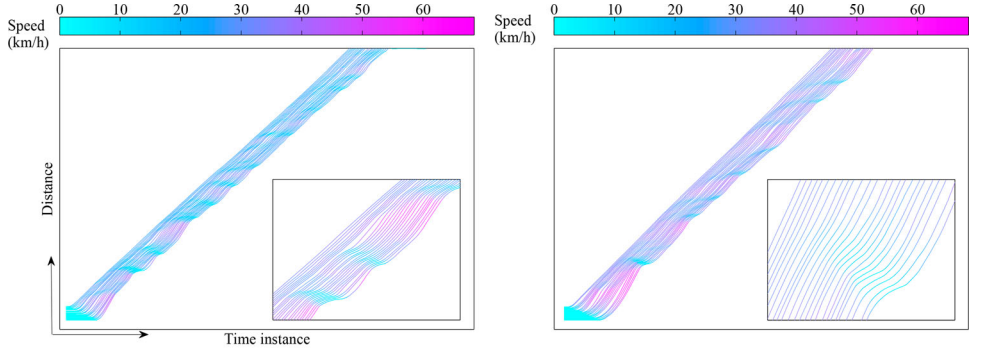

(a) $v_{\text{lead}} = 25$ km/h (b) $v_{\text{lead}} = 35$ km/h

Figure 4. Samples of vehicular trajectories in car-following experiments. The experiments have been reported in Jiang et al. (2014, 2015). Without lane changing, oscillations can be observed. The subfigure at the right corner of each figure shows the formation and the development of oscillations. (a) $v_{\text{lead}} = 25$ km/h. (b) $v_{\text{lead}} = 35$ km/h.

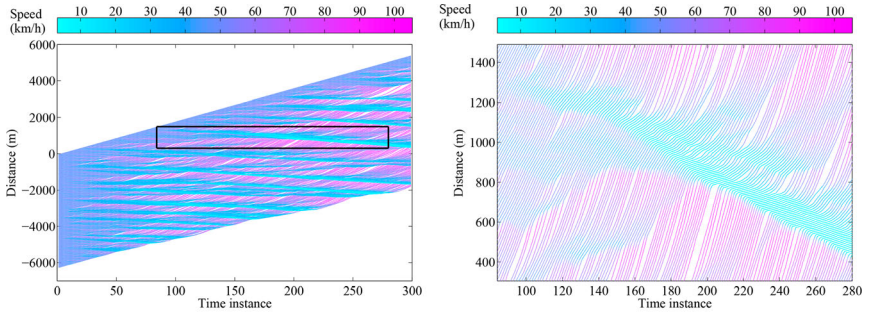

(a) $v_{\text{lead}} = 50$ km/h (b) A zoomed-in version of trajectories in the rectangle.

Figure 5. Samples of vehicular trajectories in simulations. The color map indicates the vehicular speed. $v_{\text{lead}} = 50$ km/h in this sample. An overview of the simulation results are given in (a). The trajectories in the rectangle in (a) is shown in (b) for a better visualization. In simulations, $\beta = 0.06$ and $\sigma = 0.06$. (a) $v_{\text{lead}} = 50$ km/h. (b) A zoomed-in version of trajectories in the rectangle.

3.1. Platoon oscillation growth

Empirical data show that the standard deviation of vehicular speeds in a platoon with a constant-speed leader increases along the platoon in a concave way. This 'concavity' in the oscillation growth was first revealed in a 25-vehicle car-following platoon experiment (Jiang et al. 2014); Figure 4 shows two sample experiments. Tian et al. (2016) used both Jiang's and NGSIM trajectory data and found that when the leader speed is in between 30 and 55 km/h, the oscillation growth is well approximated by a single concave function. These findings are consistent with Li and Ouyang (2011), who show that oscillation amplitude exhibits a similar growth pattern. But this reference also shows that as of vehicle number increases oscillation amplitude standard stabilizes, something not seen in Jiang's data.

Our simulation experiment consists of a 250-vehicle platoon on a one-lane road. The platoon leader drives at a constant speed v_{lead}, which is set to be 30, 40 and 50 km/h in different simulations. For each value of v_{lead}, we run 500 simulations, each for $T = 300\tau$ long. For comparison purposes, we use different values of β and σ. At time $t = 0$, all vehicles are driving in a congested state with an equilibrium spacing $1/\rho_0$. ρ_0 is the density in the congestion. That is, $v_i(0) = w(\rho_j - \rho_0)/\rho_0, i = 1, 2, \ldots 250$.

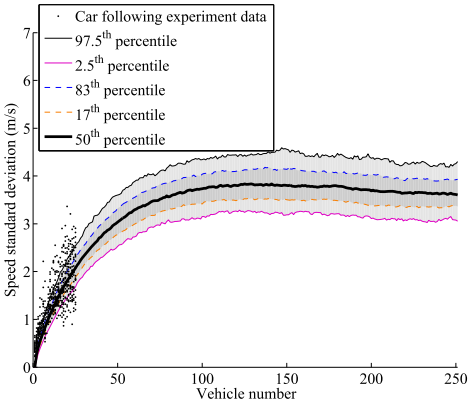

(a) Concavity with $v_{\text{lead}} = 30$ km/h.

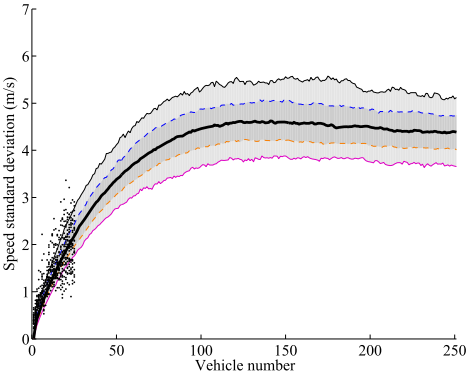

(b) Concavity with $v_{\text{lead}} = 40$ km/h.

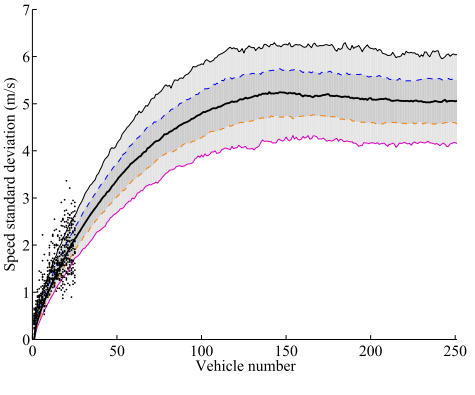

(c) Concavity with $v_{\text{lead}} = 50$ km/h.

Figure 6. Concavity revealed in car-following platoon simulations when the leading vehicle in the platoon drives at (a) $v_{\text{lead}} = 30$ km/h, (b) $v_{\text{lead}} = 40$ km/h and (c) $v_{\text{lead}} = 50$ km/h. We used $\beta = 0.06$ and $\sigma = 0.055$. The shaded areas illustrate the 95%-percentage (between 97.5th and 2.5th percentile) and 66%-percentage (between 83th and 17th percentile) of the 500 simulations. The bold curve is the mean value of the simulation results. The dots in Figure 6 are the speed standard deviation obtained from Jiangs' car-following experiments. (a) Concavity with $v_{\text{lead}} = 30$ km/h. (b) Concavity with $v_{\text{lead}} = 40$ km/h. (c) Concavity with $v_{\text{lead}} = 50$ km/h.

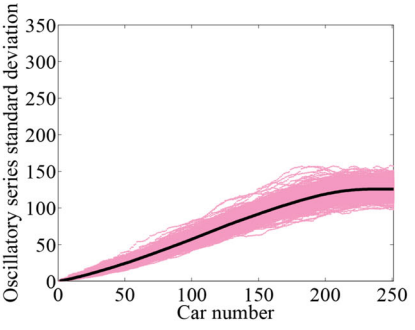

(a) Standard deviation of oscillatory series with $v_{\text{lead}} = 30$ km/h.

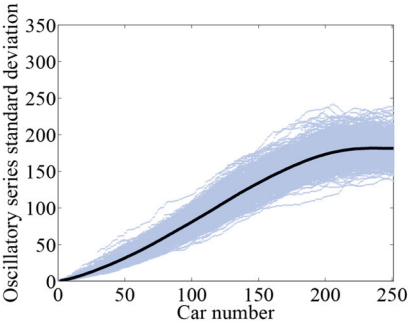

(b) Standard deviation of oscillatory series with $v_{\text{lead}} = 40$ km/h.

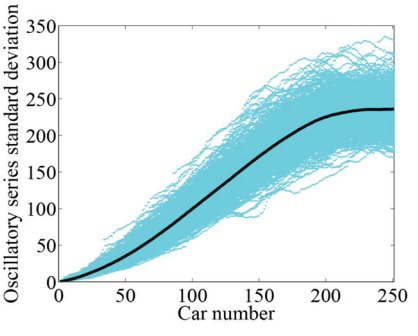

(c) Standard deviation of oscillatory series with $v_{\text{lead}} = 50$ km/h.

Figure 7. Standard deviation of oscillatory series revealed in car-following platoon simulations when the leading vehicle in the platoon drives at (a) $v_{\text{lead}} = 30$ km/h, (b) $v_{\text{lead}} = 40$ km/h and (c) $v_{\text{lead}} = 50$ km/h. In simulations, $\beta = 0.06$ and $\sigma = 0.055$. (a) Standard deviation of oscillatory series with $v_{\text{lead}} = 30$ km/h. (b) Standard deviation of oscillatory series with $v_{\text{lead}} = 40$ km/h. (c) Standard deviation of oscillatory series with $v_{\text{lead}} = 50$ km/h.

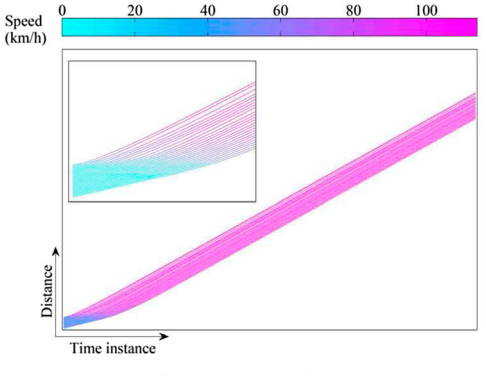

(a) $v_j = 50$ km/h

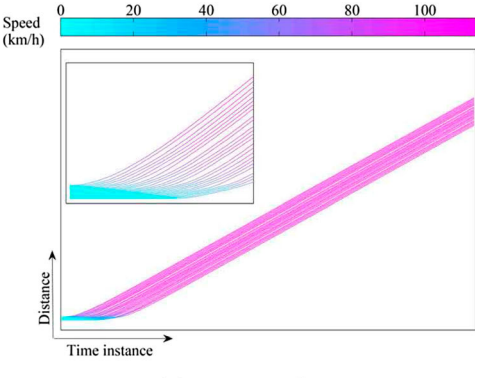

(b) $v_j = 0$ km/h.

Figure 8. Sample trajectories from our simulations. The color map indicates the vehicular speed. The speed at $t = 0$ is (a) $v_j = 50$ km/h (or density$\rho_0 = 39$ veh/km) and (b) $v_j = 0$ km/h (or density $\rho_0 = \rho_j \approx 146.7$ veh/km). $N = 50$ vehicles, excluding the virtual vehicle, are simulated on a one-lane road segment. (a) $v_j = 50$ km/h. (b) $v_j = 0$ km/h.

The sample trajectories in Figure 5 show how several oscillations develop and grow. Figure 6 shows the relation between the vehicle number and the distribution of speed standard deviation obtained from the 500 simulation runs. The v_{lead} increases from Figure 6(a) to Figure 6(c). It can be seen that

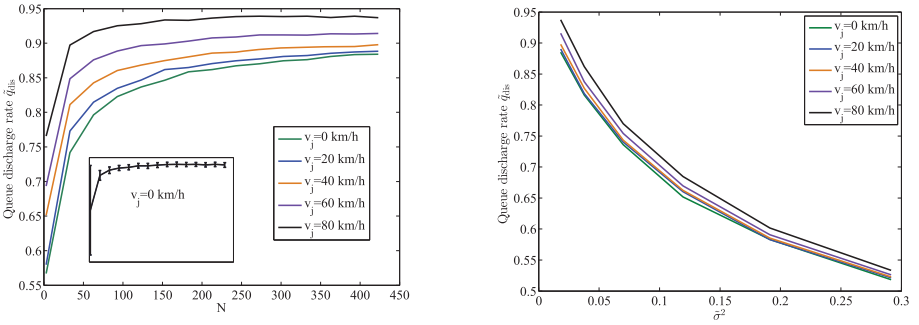

(a) Sensitive analyses of parameter N with constant $\beta = 0.07\text{s}^{-1}$ and $\sigma = 0.05\text{s}^{-1/2}$.

(b) Sensitive analyses of parameter $\tilde{\sigma}^2$ with $\beta = 0.07\text{s}^{-1}$ and $N = 441$ veh.

Figure 9. Simulation results by means of observed queue discharge rates as a function of parameter N and $\tilde{\sigma}^2$. (a) Sensitive analyses of parameter N with constant $\beta = 0.07\text{s}^{-1}$ and $\sigma = 0.05\text{s}^{-1/2}$. (b) Sensitive analyses of parameter $\tilde{\sigma}^2$ with $\beta = 0.07\text{s}^{-1}$ and $N = 441$ veh.

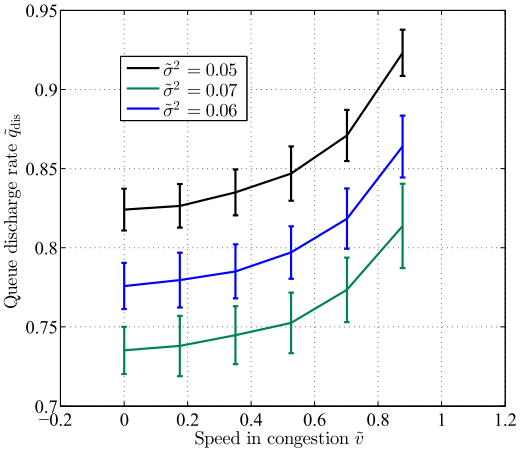

Figure 10. Relation between the speed in congestion and the capacity drop given by the extended parsimonious car-following model. The error bar indicates the standard variance of the queue discharge rate.

the standard deviation of vehicular speed increases in a concave curve along the platoon when the car number is small, e.g. smaller than 100. As the vehicle number increases, the standard deviation of speed flattens out around a fixed value, which itself increases with v_{lead}.The good match with empirical data is apparent.

Figure 7 shows how the standard deviation of oscillatory series $\hat{x}(t) = x(t) - \bar{x}(t)$ propagate along the platoon. $\bar{x}(t)$ can be seen as the Newell's trajectory. A growing-and-flattening pattern can be observed, which is consistent with Li and Ouyang (2011). In addition, we observed that the standard variance of the oscillatory series stabilize at a fixed value, which is withv_{lead}.

3.2. Speed-capacity relationship

In this section, we study to what extent the proposed model can reproduce the speed-capacity relationship observed in Yuan, Knoop, and Hoogendoorn (2015) and Oh and Yeo (2015). As observed in Oh and Yeo (2015), the queue discharge rate reduction in absence of lane changing is a large proportion of the reduced capacity at bottlenecks, outperforming the reduction due to lane changing.

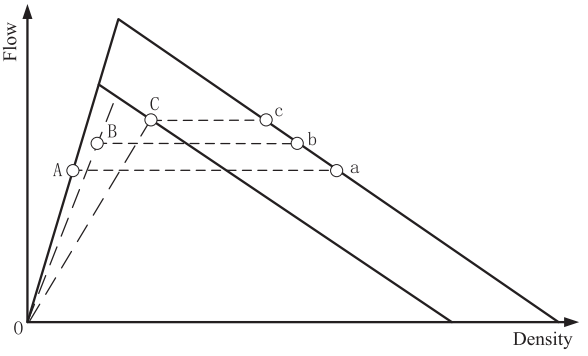

Figure 11. As the speed limit downstream of a lane drop bottleneck can increase the queue discharge rate.

The simulation setup in this section is identical to the previous sections. But the leading vehicle which drives at a low constant speed v_{lead}, is removed, allowing vehicles in the queue to accelerate.

Figure 8 shows two sample runs from our simulations. It can be seen that as vehicle accelerate voids appear within the platoon, which propagate indefinitely downstream, causing the capacity drop. To measure this drop, we calculate the queue discharge flow q_{dis} per:

$$q_{\text{dis}} = \frac{(N-1)\, v_f}{\sum_{i=2}^{N} s_i(T)} \tag{8}$$

where $s_i(T)$ is vehicle i's spacing at the simulation ending time T, and N is the number of vehicles in the platoon. A dimensionless queue discharge rate $\tilde{q}_{\text{dis}}$ is used in coming analysis, with unit C. We selected $N = 450$ since we observed that the discharge rate stabilizes at that point; see Figure 9(a).

Figure 9(b) shows the queue discharge rate is a decreasing linear function of $\tilde{\sigma}$. A decreasing function is as expected because the larger the viability of the acceleration processes, the larger the voids in the traffic stream; linearity is somewhat surprising.

Finally, Figure 10 shows that the proposed model produces a speed-capacity relationship that is consistent with empirical data. Notice that if $\tilde{\sigma}^2 = 0.06$, the capacity drop can reach around 22% with a wide moving jam (i.e. $v_j = 0$ km/h), which is similar to the capacity drop magnitude empirically observed in Yuan, Knoop, and Hoogendoorn (2015) and Yuan, Knoop, and Hoogendoorn (2017a).

4. Conclusions and discussions

There are two relevant contributions in this work. Firstly, this paper for the first time proposes a longitudinal behavior-oriented interpretation - desired acceleration errors - to explain the capacity drop. Though numerous car-following models in literature have been able to reproduce the queue discharge rate reduction and (possibly) even the speed-capacity relation, we argue that the approach used in those models lacks a connection with driver behavior. That is, a profound behavioral mechanism which can even interpret the mechanisms (as introduced in Section 1) proposed in those previous car-following models is desirable. Our first contribution is such an attempt. It is worthwhile to notice that the desired acceleration error mechanism originates from empirical observations.

Secondly, this paper extended the parsimonious car-following model in Laval, Toth, and Zhou (2014) to reproduce empirical speed-capacity relationships. This was achieved by modeling driver acceleration errors as a Geometric Brownian motion, which is consistent with our empirical data showing that the standard deviation of the desired acceleration is a decreasing function of the speed. It is worthwhile to notice that the desired acceleration error mechanism seems to be operational nowadays. The possible implications for traffic management are discussed in this section later.

Notably, the extended model remains a single-parameter model if one is interested in flow or delay calculations; in particular, the speed-capacity relationship depends on a single parameter, $\tilde{\sigma}^2 = \sigma^2/\beta$. Similarly, the queue discharge rate was found to be a decreasing linear function of $\tilde{\sigma}$. From the driver behavior perspective, this parameter encapsulates human error, σ^2 and how fast acceleration changes with speed, β. Therefore, queue discharge rates can be increased by (i) decreasing human error as much as possible, especially at the beginning of the acceleration process, and/or (ii) increasing the acceleration at low speeds, by increasing engine power and/or educating drivers to be more aggressive when accelerating from a full stop.

Based on these findings, firstly we can argue that newer vehicle technologies should be beneficial for reducing or maybe even eliminating capacity drop. Autonomous vehicles should be able to substantially reduce the variability of acceleration processes, which is consistent with (i) above; electric vehicles offer much greater accelerating power than conventional combustion engine vehicles, especially at lower speeds, which accords well with (ii). Secondly, the roadside traffic management can also gain benefits from our findings, which again differs from previous car-following models. Let us give an example. Yuan, Knoop, and Hoogendoorn (2015) show a lane drop on A4 in the Netherlands where serious congestion have been observed for several days. If we set a speed limit – say 70 km/h – in the downstream of the lane drop, then we believe that the queue discharge rate can be increased since the β increases which decreases the $\tilde{\sigma}$. In Figure 11, the capitals indicate the traffic state downstream of the lane-drop bottleneck, while the lower cases indicate the congested state upstream. Without the speed limit, the queue discharge rate corresponds to state 'A' and 'a'. When speed limit is conducted, in Figure 11 the free-flow speed decreases from v_{OA} to v_{OB} (v_{OA}, v_{OB} and v_{OC} is the slope of line OA, OB and OC, respectively), the queue discharge rate increase from q_a to q_b. q_a, q_b and q_c correspond to state 'a', 'b' and 'c' respectively. Finally, when the speed limit reduces to v_{OC} when the flow in state C equals q_c, we believe that v_{OC} can be the optimal speed limit.

It is worthwhile to notice that the fundamental diagram used in this study is triangular. One may argue that the triangular fundamental diagram is an approximation rather than reality. But the shape of the fundamental diagram will not influence the acceleration model at all. In the acceleration model, the only parameter associated to the fundamental diagram is the free-flow speed which will be given in a FD with any shapes.

We used the comprehensive car-following experiment in Jiang et al. (2014) to show that the model also captures the 'concavity' in traffic flow. Further analysis is needed to investigate if concavity in our model also depends on the fundamental diagram parameters, and if it is able to produce the periods and amplitudes of oscillations observed in the data. More data calibrations and validations of the model in freeway environment are desirable. These topics are currently being investigated by the authors (e.g. Xu and Laval 2018).

The desired acceleration model (see Section 2.1) developed in this paper can be incorporated into the OVM (Optimal Velocity Model) or IDM (Intelligent Driver Model) car-following model in a straightforward way when describing the acceleration on a free road from a standstill (i.e. we don't need to use the adaptation time in the IDM and OVM car-following model. Readers are referred to Treiber and Kesting (2013) for descriptions on the OVM and IDM car-following model).

The primary interest of this research is in the longitudinal driving behavioral mechanism behind the capacity drop. The model developed in this paper contributes to validating the proposed mechanism. In the future, to what extent this model can reproduce or/and explain other traffic phenomena should be investigated. Moreover, for operation more consideration of the uncertainty and stochasticity in traffic flow should be desirable.

Acknowledgments

This study has received funding from NSF research project # 1055694, NWO grant 'there is plenty of room in the other lane' and CSC scholarship.

Disclosure statement

No potential conflict of interest was reported by the authors.

Funding

This study has received funding from research project # 1055694, the Netherlands Organisation for Scientific Research (NWO) grant 'there is plenty of room in the other lane' and China Scholarship Council (CSC) scholarship.

ORCID

Serge P. Hoogendoorn http://orcid.org/0000-0002-1579-1939

References

Allen, R., D. Harwood, J. Chrstos, and W. Glauz. 2000. "The Capability and Enhancement of vdanl and twopas for Analyzing Vehicle Performance on Upgrades and Downgrades within ihsdm." FHWA Publication No. 00-078.

Banks, J. H. 1991. "The Two-Capacity Phenomenon: Some Theoretical Issues." *Transportation Research Record* 1320: 234–241.

Cassidy, M. J., and R. L. Bertini. 1999. "Some Traffic Features at Freeway Bottlenecks." *Transportation Research Part B: Methodological* 33: 25–42.

Cassidy, M. J., and J. Rudjanakanoknad. 2005. "Increasing the Capacity of an Isolated Merge by Metering Its On-Ramp." *Transportation Research Part B: Methodological* 39: 896–913.

Chen, D., S. Ahn, S. Bang, and D. Noyce. 2016. "Car-following and Lane-changing Behavior Involving Heavy Vehicles." Proceedings of Transportation Research Board 95th Annual Meeting, Washington, DC.

Chen, D., S. Ahn, J. Laval, and Z. Zheng. 2014. "On the Periodicity of Traffic Oscillations and Capacity Drop: The Role of Driver Characteristics." *Transportation Research Part B: Methodological* 59: 117–136.

Chen, D., J. A. Laval, S. Ahn, and Z. Zheng 2012b. "Microscopic Traffic Hysteresis in Traffic Oscillations: A Behavioral Perspective." *Transportation Research Part B: Methodological* 46: 1440–1453.

Chen, D., J. Laval, Z. Zheng, and S. Ahn. 2012a. "A Behavioral Car-Following Model that Captures Traffic Oscillations." *Transportation Research Part B: Methodological* 46: 744–761.

Chung, K., J. Rudjanakanoknad, and M. J. Cassidy 2007. "Relation Between Traffic Density and Capacity Drop at Three Freeway Bottlenecks." *Transportation Research Part B: Methodological* 41: 82–95.

Coifman, B.. 2015. "Empirical Flow-Density and Speed-Spacing Relationships: Evidence of Vehicle Length Dependency." *Transportation Research Part B: Methodological* 78: 54–65.

Coifman, B., and S. Kim. 2011. "Extended Bottlenecks, the Fundamental Relationship, and Capacity Drop on Freeways." *Procedia – Social and Behavioral Sciences* 17: 44–57.

Daganzo, C. F., and V. L. Knoop. 2016. "Traffic Flow on Pedestrianized Streets." *Transportation Research Part B: Methodological* 86: 211–222.

Hall, F. L., and K. Agyemang-Duah. 1991. "Freeway Capacity Drop and the Definition of Capacity." *Transportation Research Record* 1320: 91–98.

Jiang, R., M. B. Hu, H. Zhang, Z. Y. Gao, B. Jia, and Q. S. Wu. 2015. "On Some Experimental Features of Car-following Behavior and How to Model Them." *Transportation Research Part B: Methodological*80: 338–354.

Jiang, R., M. B. Hu, H. M. Zhang, Z. Y. Gao, B. Jia, Q. S. Wu, B. Wang, and M. Yang. 2014. "Traffic Experiment Reveals the Nature of Car-Following." *PLoS ONE* 9: e94351.

Laval, J. A., and B. R. Chilukuri. 2016. "Symmetries in the Kinematic Wave Model and a Parameter-Free Representation of Traffic Flow." *Transportation Research Part B Methodological* 89: 168–177.

Laval, J. A., and C. F. Daganzo. 2006. "Lane-Changing in Traffic Streams." *Transportation Research Part B: Methodological* 40: 251–264.

Laval, J. A., and L. Leclercq. 2010. "A Mechanism to Describe the Formation and Propagation of Stop-and-Go Waves in Congested Freeway Traffic." *Philosophical Transactions of the Royal Society of London A: Mathematical, Physical and Engineering Sciences* 368: 4519–4541.

Laval, J. A., C. S. Toth, and Y. Zhou. 2014. "A Parsimonious Model for the Formation of Oscillations in Car-following Models." *Transportation Research Part B: Methodological* 70: 228–238.

Leclercq, L., V. L. Knoop, F. Marczak, and S. P. Hoogendoorn. 2015. "Capacity Drops at Merges: New Analytical Investigations." *Transportation Research Part C: Emerging Technologies* 62: 171–181.

Leclercq, L., J. A. Laval, and N. Chiabaut. 2011. "Capacity Drops at Merges: An Endogenous Model." *Transportation Research Part B: Methodological* 45: 1302–1313.

Li, X., and Y. Ouyang. 2011. "Characterization of Traffic Oscillation Propagation Under Nonlinear Car-Following Laws." *Transportation Research Part B: Methodological* 45: 1346–1361.

Lighthill, M. J., and G. B. Whitham. 1955. "On Kinematic Waves. II. A Theory of Traffic Flow on Long Crowded Roads." *Proceedings of the Royal Society of London A: Mathematical, Physical and Engineering Sciences* 229: 317–345.

Newell, G. 2002. "A Simplified Car-Following Theory: A Lower Order Model." *Transportation Research Part B: Methodological* 36: 195–205.

Oh, S., and H. Yeo. 2015. "Impact of Stop-and-Go Waves and Lane Changes on Discharge Rate in Recovery Flow." *Transportation Research Part B: Methodological* 77: 88–102.

Øksendal, B. 2010. *Stochastic Differential Equations: An Introduction with Applications*. New York: Springer.

Papageorgiou, M., I. Papamichail, A. Spiliopoulou, and A. Lentzakis. 2008. "Real-Time Merging Traffic Control with Applications to toll Plaza and Work Zone Management." *Transportation Research Part C: Emerging Technologies* 16: 535–553.

Richards, P. I. 1956. "Shock Waves on the Highway." *Operations Research* 4: 42–51.

Srivastava, A., and N. Geroliminis. 2013. "Empirical Observations of Capacity Drop in Freeway Merges With Ramp Control and Integration in a First-Order Model." *Transportation Research Part C: Emerging Technologies* 30: 161–177.

Tampère, C. 2004. "Human-kinetic Multiclass Traffic Flow Theory and Modelling with Application to Advanced Driver Assistance Systems in Congestion." Ph.D. thesis, Delft University of Technology.

Tian, J., R. Jiang, B. Jia, Z. Gao, and S. Ma. 2016. "Empirical Analysis and Simulation of the Concave Growth Pattern of Traffic Oscillations." *Transportation Research Part B: Methodological* 93: 338–354.

Treiber, M., A. Hennecke, and D. Helbing. 2000. "Congested Traffic States in Empirical Observations and Microscopic Simulations." *Physical Review E* 62: 1805–1824.

Treiber, M., and A. Kesting. 2013. *Traffic Flow Dynamics: Data, Models and Simulation*. Berlin: Springer.

Treiber, M., A. Kesting, and D. Helbing. 2006. "Understanding Widely Scattered Traffic Flows, the Capacity Drop, and Platoons as Effects of Variance-Driven Time Gaps." *Physical Review E* 74: 016123

Wong, G., and S. Wong. 2002. "A Multi-Class Traffic Flow Model – An Extension of LWR Model with Heterogeneous Drivers." *Transportation Research Part A: Policy and Practice* 36: 827–841.

Wu, C. X., P. Zhang, S. Wong, and K. Choi. 2014. "Steady-State Traffic Flow on a Ring Road With up- and Down-Slopes." *Physica A: Statistical Mechanics and its Applications* 403: 85–93. URL: http://www.sciencedirect.com/science/article/pii/S0378437114001174.

Xu, T., and J. A. Laval. 2018 "Parameter Estimation of a Stochastic Microscopic Car-following Model." Proceedings of Transportation Research Board 97th Annual Meeting.

Yeo, H. 2008 "Asymmetric Microscopic Driving Behavior Theory." Ph.D. thesis, University of California Transportation Center, UC Berkeley: University of California Transportation Center.

Yuan, K. 2016. "Capacity Drop on Freeways: Traffic Dynamics, Theory and Modeling." Phd thesis, Delft University of Technology.

Yuan, K., V. L. Knoop, and S. P. Hoogendoorn. 2015. "Capapcity Drop: A Relation Between the Speed in Congestion and the Queue Discharge Rate." *Transportation Research Record: Journal of the Transportation Research Board* 2491: 72–80.

Yuan, K., V. L. Knoop, and S. P. Hoogendoorn. 2017a. "A Microscopic Investigation into the Capacity Drop: Impacts of Longitudinal Behavior on the Queue Discharge Rate." *Transportation Science* 51: 852–862

Yuan, K., V. L. Knoop, L. Leclercq, and S. P. Hoogendoorn. 2017b. "Capacity Drop: A Comparison Between Stop-and-Go Wave and Standing Queue at Lane-Drop Bottleneck." *Transportmetrica B: Transport Dynamics* 5: 149–162. http://dx.doi.org/10.1080/21680566.2016.1245163.

Zhang, H., and T. Kim. 2005. "A Car-Following Theory for Multiphase Vehicular Traffic Flow." *Transportation Research Part B: Methodological* 39: 385–399.

Zhang, P., C. X. Wu, and S. Wong. 2012. "A Semi-Discrete Model and Its Approach to a Solution for a Wide Moving Jam in Traffic Flow." *Physica A: Statistical Mechanics and its Applications* 391: 456–463.